

Sensitivity of Marching Modulus of silica-filled SBR/BR compounds  
to filler type and polymer ratio

W.K. Dierkes\*, University of Twente, Enschede,  
The Netherlands

J. Jin<sup>1,2</sup>, J.W.M. Noordermeer<sup>1</sup>, A. Blume<sup>1</sup>

<sup>1</sup> University of Twente, Enschede, The Netherlands

<sup>2</sup> HANKOOKTIRE Co., LTD. Main R&D Center, Republic of Korea

Presented at the 198th Technical Meeting  
of the Rubber Division, ACS  
Knoxville, TN, October 20-22, 2020

ISSN: 1547-1977

## ABSTRACT

Silica-silane filler systems are very successful in passenger car tire treads as they considerably improve tire performance, mainly rolling resistance. However, this technology has its drawbacks in terms of processing: longer mixing cycles, two or three mixing stages, as well as influences on the curing behavior of the compound. One specific problem related to the latter is a marching modulus, which makes determination of the correct curing time difficult. As a consequence, the properties of silica compounds might vary. In this study, the influence of polymer ratio as well as dispersibility of silica on the curing kinetics is investigated.

The polymers used in general with a silica-silane filler system in tread compounds are sSBR and BR, and the ratio of these two polymers significantly influences curing behavior as well as marching modulus. This is a consequence of differences in compatibility of the filler with the two polymers, and in reactivity of the two polymers to form sulfur bonds.

The dispersibility of the silica is also expected to influence the curing kinetics due to differences in relative surface area and in interaction with the curatives. However, when comparing different silica grades, no significant influence on marching modulus was found.

## INTRODUCTION

Due to thermodynamic considerations, elastomer blends are often heterogeneous on micro- and nano-scale and show a certain phase morphology according to the level of miscibility of the blended species.<sup>1-4</sup> Further, each type of elastomer has its own specific affinity to reinforcing fillers, silica in the present case.<sup>4,5</sup> Wang and Wolff compared the affinity of model chemical probes representing elastomers and found, that the degree of interaction of rubber with silica fillers varies in the following order: Nitrile butadiene rubber (NBR) > Styrene Butadiene Rubber > Natural Rubber (NR) > Butadiene Rubber > Ethylene Propylene Diene polyMethylene Rubber (EPDM) > Butyl Rubber (IIR).<sup>6</sup> Le et al. reported that the nature of the rubber-filler interactions strongly affects the filler surface wetting behavior.<sup>5,7,8</sup> In turn, this will also have an influence on the flocculation behavior: the tendency of the silica filler to demix after having been mixed. Stöckelhuber reported that flocculation can be reduced by a higher compatibility between rubber and filler surface.<sup>9</sup> These studies imply that the characteristics of the materials such as the chemistry of the polymer and the filler surface, are recognized as crucial factors for filler dispersion and network formation during vulcanization.<sup>10-14</sup>

Beside of the polymer characteristics, the dispersibility of silica – defined as the ability of the filler to be homogeneously distributed as small clusters in a rubber matrix<sup>15</sup> – is a strong influencing factor for the final dispersion quality in a rubber matrix.<sup>16,17</sup> Blume and Uhrlandt<sup>16</sup> compared the dispersion behavior of conventional (CV) and Highly Dispersible (HD) silicas by using laser diffraction after ultrasonic treatment of suspensions of these silicas, and found enhanced silica cluster fragmentation for HD silica.

In order to confirm the effect of incompatible SBR/BR blend ratios as well as the dispersibility of silicas on factors affecting the marching modulus – the phenomenon that during vulcanization no plateau profile or constant modulus is reached within acceptable time scale – of silica filled compounds, two series of experimental sets are performed within the present study.

- Series 1: the results are interpreted in terms of the degree of silanization, and also concerning the chemical structure of SBR and BR, their cis/trans and 1,2-vinyl butadiene units and their respective reactivities;
- Series 2: The dispersibility of these silicas, with and without silane coupling agent, is compared in terms of macro- and micro-dispersion. Additionally, the factors affecting the marching modulus as well as the amount of bound rubber are evaluated and correlated to the former.

## EXPERIMENTAL

### MATERIALS

All series of experiments were done based on a tire tread compound as shown in Tables I and II. Blends of oil-extended solution styrene-butadiene rubber (S-SBR, Mooney viscosity (ML1+4@100°C) of 65 and composed of 75% butadiene with a vinyl-content of 50%, and 25% styrene-content, extended with 37.5 phr of TDAE oil), and high cis-1,4 polybutadiene rubber (BR, Mooney viscosity (ML1+4@100°C) of 44 and a cis-1,4 content of 96%) were used in this study. The classification of the different types of silica, as Conventional silica (CV) and Highly-Dispersible (HD) silica, is listed in Table III. Bis-(triethoxysilylpropyl)tetrasulfide (TESPT) was used as silane coupling agent. The amount of TESPT applied in the formulations were adjusted according to Equation (1), based on the CTAB surface area of the silicas:<sup>18</sup>

$$TESPT (phr) = 5.3 \times 10^{-4} \times (CTAB)_{silica} \times (phr)_{silica} \quad (1)$$

The pre-blendings in Table I were prepared only for Series 1 because the S-SBR used in this work contained 27.3 wt% (or 37.5 phr) of TDAE oil whereas the BR did not contain oil. Therefore, except for SBR100 in Table I, the amount of TDAE oil for all the blends was adjusted to the same amount and introduced in the pre-blending step. 50 phr of silica – without TESPT – was introduced at the same time with TDAE oil in order to avoid slippage of the compound in the mixing chamber as well as to provide a similar amount of mixing energy for all samples.

Table I. Compound formulation for Series 1

Mixing stage	Ingredient	SBR100 [phr]	SBR80 [phr]	SBR60 [phr]	SBR50 [phr]	SBR40 [phr]	SBR20 [phr]	SBR00 [phr]
Pre-blending	S-SBR	137.6	110.0	82.5	68.8	55.0	27.5	0.0
	BR	0.0	20.0	40.0	50.0	60.0	80.0	100.0
	Silica1	50	→	→	→	→	→	→
	TDAE oil	0.0	7.6	15.1	18.8	22.6	30.1	37.6
Masterbatch	Pre-blendings	187.6	→	→	→	→	→	→
	Silica 1	50	→	→	→	→	→	→
	Silane (TESPT)	8.4	→	→	→	→	→	→
	Stearic acid	2	→	→	→	→	→	→
	Zinc Oxide	2	→	→	→	→	→	→
	DPG	1.5	→	→	→	→	→	→
Final	Masterbatches	251.5	→	→	→	→	→	→
	Sulfur	0.7	→	→	→	→	→	→
	ZBEC	0.2	→	→	→	→	→	→
	CBS	2.2	→	→	→	→	→	→

Table II Compound formulation for Series 2

Mixing stage	Ingredient	without silane		with silane	
		COM1 (phr)	COM2 (phr)	COM3 (phr)	COM4 (phr)
Master batch	S-SBR	110	→	→	→
	BR	20	→	→	→
	Silica 2	90	-	90	-
	Silica 3	-	90	-	90
	Silane (TESPT)	-	-	8.0	7.3
	TDAE oil	5	→	→	→
	Stearic acid	1	→	→	→
	Zinc oxide	2	→	→	→
	DPG	1.5	→	→	→
Final	Sulfur	0.7	→	→	→
	ZBEC	0.2	→	→	→
	CBS	2.2	→	→	→

Table III. Analytical data of silicas corresponding to Tables I and II

Sample code	Class	BET [m <sup>2</sup> /g]	CTAB [m <sup>2</sup> /g]	*OAN number [ml/100g]
Silica 1	HD Silica	180	177	223
Silica 2	CV Silica	175	167	176
Silica 3	HD Silica	155	152	205

\*Oil Absorption Number: the value represents the structure of silica. Higher number corresponds to a more developed structure

### MIXING

*Series 1.*— The details of each mixing step are shown in Tables IV and V. Before the masterbatch step, two batches of pre-blending having the same formulation were combined in order to minimize unintended variations from the pre-blending step. The fill factor for the pre-blending and masterbatch steps were fixed to 75% and 65%, respectively, limited by the maximum mechanical load capacity of the mixer. The temperature of the mixer Temperature Control Unit (TCU) was set at 50°C for the pre-blending and masterbatch steps. In order to avoid the “first batch effect”, one initial batch was mixed and discarded before the regular mixing started for both steps. In case of the masterbatch step, the rotor speed was adjusted from 04:10 (min:sec) onwards in order to reach and subsequently keep 150°C steady chamber temperature during a period of 150 seconds for silanization. After the mixing steps done in the internal mixer, the compounds were sheeted out immediately on the two-roll mill in order to cool them down and prevent further silanization as well as filler-polymer coupling reaction, in particular the masterbatch compounds. Two batches were mixed for each set of conditions in order to check the reproducibility. The final mixing stage was done by using a lab scale two-roll mill (Polymix 80T). All ingredients to vulcanize the compounds, alternatively called curatives (sulfur and curing accelerators zinc dibenzylthiocarbamate (ZBEC) and N-cyclohexyl-2-benzothiazolesulphenamide (CBS)), were added in this step.

Table IV. Pre-blending and batch fusion mixing procedures

Pre-blending		Batch fusion	
Internal mixer		Open mill	
Action	time [mm:ss]	Action	time [mm:ss]
Add polymer	00:00 ~ 00:20	Add pre-blends having the same formulation	00:00 ~ 01:00
Mastication	00:20 ~ 01:20	Milling	01:00 ~ 06:00
Silica (50 phr), TDAE oil	01:20 ~ 01:40	Discharge and separation (by weight)	-
Mixing	01:40 ~ 02:40		
Ram sweep	02:40 ~ 03:10		
Mixing	03:10 ~ 04:10		
Discharge and sheeting	-		

Table V. Masterbatch and final mixing procedures

Masterbatch		Final	
Internal mixer		Open mill	
Action	time [mm:ss]	Action	time [mm:ss]
Add fused batch	00:00 ~ 00:20	Add masterbatch	-
Mixing	00:20 ~ 01:20	Mixing	00:00 ~ 02:00
Silica (50 phr), silane, remaining ingredients	01:20 ~ 01:40	Add curatives	02:00 ~ 02:30
Mixing	01:40 ~ 02:40	Mixing	02:30 ~ 09:00
Ram sweep	02:40 ~ 03:10	Discharge	-
Mixing till 150°C	03:10 ~ 04:10		
Ram sweep	04:10 ~ 04:14		
Mixing at 150°C	04:14 ~ 06:40		
Discharge and sheeting	-		-

*Series 2.* — Both COM1 and 2 were mixed with 150 seconds of hold time. COM3 and 4 were mixed with 50, 150 and 250 seconds of silanization time. The fill factor of the internal mixer was fixed at 63%. Except the fill factor, the same mixer, TCU condition, silanization temperature control technique are applied to Series 2.

Table VI. Masterbatch and final mixing procedures

Masterbatch		Final	
Internal mixer		Open mill	
Action	time [mm:ss]	Action	time [mm:ss]
Add polymer	00:00 ~ 00:20	Add masterbatch	-
Mixing	00:20 ~ 01:20	Mixing	00:00 ~ 02:00
½ Silica, silane (COM3 and 4 only)	01:20 ~ 01:40	Add curatives	02:00 ~ 02:30
Mixing	01:40 ~ 02:40	Mixing	02:30 ~ 09:00
Ram sweep	02:40 ~ 03:10	Discharge	-
Mixing till 150°C	03:10 ~ 04:10		
Ram sweep	04:10 ~ 04:14		
Mixing for various time laps: 0, 150, 250 sec	04:14 ~ 06:40		
Discharge and sheeting	-		-

#### MICRO-DISPERSION OF SILICA BY PAYNE EFFECT

The Payne effect of the uncured rubber compounds were evaluated by using a Rubber Process Analyzer (RPA; RPA Elite, TA Instruments). The storage shear moduli ( $G'$ ) were measured at a temperature of 100°C, a frequency of 0.5 Hz and varying strains in the range of 0.56 - 200%. The Payne effect values were calculated from the difference in storage shear moduli at low strain (0.56%) and high strain (100%), i.e.  $G'(0.56\%) - G'(100\%)$ .

#### MACRO-DISPERSION OF SILICA BY DISPERGRADER

The EVONIK topography test was chosen for macro-dispersion assessment of the compounds. The images obtained from the measurement and the amount of undispersed silica clusters larger than 2  $\mu\text{m}$  were used for the indication of macro-dispersion. This method can measure the macro-dispersion of fillers by scanning a freshly cut surface of a cured rubber sample based on ASTM D2663 – Method C.<sup>19</sup> In total, one hundred diamond tips having 5  $\mu\text{m}$  of radius slide over 5mm<sup>2</sup> of the cut surface and detect the irregularities, which represent the undispersed filler clusters. Subsequently, the surface roughness is analyzed by a special software, giving information on surface roughness, number of undispersed silica clusters and others.<sup>17</sup> Additionally, a grey shades image can be obtained by converting the roughness of the cut sample surface.<sup>16,17</sup> For this study, the measurements were done by the R&D center of Evonik Resource Efficiency GmbH (Wesseling, Germany).

#### FILLER FLOCCULATION RATE

The Filler Flocculation Rate (FFR) of the uncured compounds from the masterbatch step was studied by using the RPA mentioned above at 100°C, a strain of 0.56% and test time of 14 minutes including 2 minutes of pre-heating time. The measurement temperature was selected according to a typical industrially employed extrusion temperature. The storage shear moduli were recorded at different measurement times. According to Mihara et al. it is possible to observe the flocculation of silica particles by monitoring the change of storage modulus ( $G'$ ) at low strain under isothermal conditions.<sup>20</sup> The results can best be fitted with Equation 2:<sup>21,22</sup>

$$FFR = \frac{d \log \left( G'_{0.56}(t) / G'_{0.56i} \right)}{d \log \left( t / t_i \right)} \quad (2)$$

Where FFR is a dimensionless flocculation rate,  $G'_{0.56}(t)$  is the storage modulus at 0.56% strain at time  $t$ ; Equation 2 is normalized with  $G'_{0.56i}$ , the initial storage modulus at  $t_i$ , and  $t_i$  is 1 minute.

#### FILLER-POLYMER COUPLING RATE

The filler-polymer Coupling Rate (CR) of the uncured compounds from the masterbatch step was studied by using the RPA under the following conditions: 160°C, 1.677 Hz and 3 degrees (~42% of strain) for 40 minutes. A large strain was applied for the CR measurements in order to break the filler-filler interaction. Therefore, only the filler-polymer interaction is taken into account in the CR. After the torque levels at different times were recorded and normalized, CR was calculated following Equation 3, based on a same concept as Equation 2:<sup>21,22</sup>

$$CR = \frac{d \log \left( T(t) / T_{scorch} \right)}{d \log \left( t / t_{scorch} \right)} \quad (3)$$

Where CR is the dimensionless filler-polymer coupling rate,  $T(t)$  is the torque level at test time  $t$ ,  $T_{scorch}$  is the torque level at  $t_{scorch}$ , the time to incipient cure or scorch which corresponds to the time for the torque to increase by 1 (dN·m):  $T(t) = T_{min} + 1$  (dN·m).  $T_{min}$  is the minimum torque level which is observed during the measurement.

#### CURE CHARACTERISTICS AND MARCHING MODULUS INTENSITY

The rheograms of the compounds after the final mixing step were measured at 160°C for 40 minutes under two different strain conditions as follows:

- 0.5 degrees (~7% of strain) and a frequency of 1.667 Hz: ASTM D5289-95,<sup>23</sup>
- 3 degrees (~42% of strain) and a frequency of 1.667 Hz.

The Marching Modulus Intensity (MMI) was calculated from the rheograms by using **Equation 4**:<sup>21,22</sup>

$$MMI = \frac{T_{40} - T_{20}}{40min - 20min} \quad (4)$$

Where  $MMI$  is the marching modulus intensity,  $T_{40}$  and  $T_{20}$  are the corresponding torques at 40 minutes and 20 minutes.

#### BOUND RUBBER CONTENT

Approximately 0.2 g of the rubber compounds without curatives, as obtained from the masterbatch step, were cut into small pieces and immersed in toluene at room temperature for 5 days, while the toluene was



renewed every day. Thereafter, the samples were removed from the toluene, dried at 105°C for 24 h and weighed. Total bound rubber content was calculated according to Equation 5:<sup>24</sup>

$$\text{Bound rubber content (\%)} = \frac{W_{fg} - W \left( \frac{m_f}{m_f + m_p} \right)}{W \left( \frac{m_p}{m_f + m_p} \right)} \times 100 \quad (5)$$

Where  $W_{fg}$  is the weight of filler plus gel,  $W$  is the original weight of the specimen, and  $m_f$  and  $m_p$  are the weights of filler and polymer in the compound, respectively.

The degree of filler-polymer coupling can be measured by the chemically bound rubber content. For this analysis, approximately 0.2 g of the rubber compounds without curatives, as obtained from the masterbatch step, were cut into small pieces and immersed in toluene at room temperature for 5 days, this time under ammonia atmosphere in order to cleave physical linkages. The toluene was renewed every day. Then, the samples were removed from the toluene, dried at 105°C for 24 h and weighed. The chemically bound rubber content was calculated according to Equation 5. The physically bound rubber content was calculated by subtraction of the chemically bound rubber content from the total bound rubber content.

### VULCANIZATION

Vulcanization of the compounds from the final mixing step was done using a Wickert laboratory press (WLP1600). The samples were vulcanized at two different cure times for solvent swelling and Mooney-Rivlin plots for Series 1 in order to be able to compare the overall crosslink density depending on the choice of the curing time of the compounds: so-called Calculated Cure Time (CCT) and a fixed time of 30 minutes. The compounds showed marching modulus behavior, therefore CCT of the compound was calculated by using a differential curve of the rheogram according to Mihara's work, as shown in Figure 1.<sup>25</sup> The time at the cross point of two tangential lines A and B of the differential curve plus 1 min was selected as CCT.

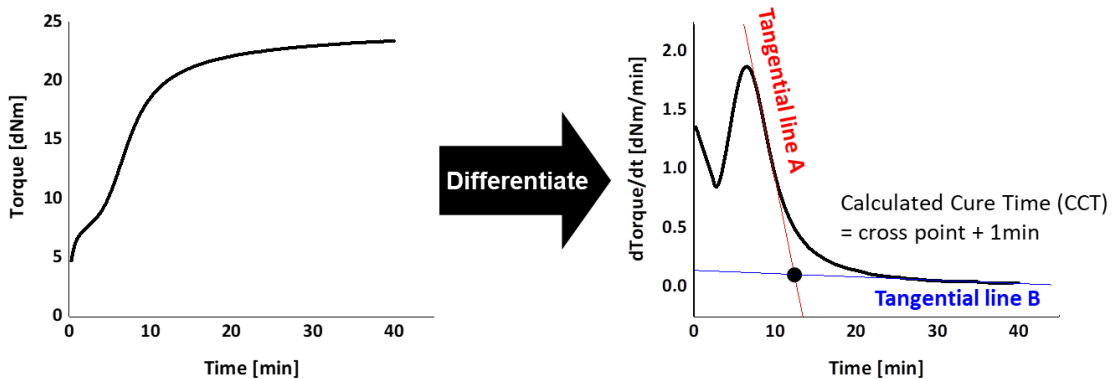


Figure 1 Cure time calculation for compounds showing marching modulus.<sup>25</sup>

### MOONEY-RIVLIN PLOT

Limited polymer chain extensibility, evaluated by the Mooney-Rivlin approach, gives additional information on the filler-polymer interaction of vulcanizates.<sup>26-31</sup> The Mooney-Rivlin formulation is given in Equation 6.<sup>[31]</sup>

$$\sigma^* = \frac{\sigma}{\lambda - \lambda^{-2}} = 2C_1 + 2C_2\lambda^{-1} \quad (6)$$

Where  $\sigma$  is the engineering stress and  $C_1$ ,  $C_2$  are constants independent of the extension ratio ( $\lambda$ ). The reduced stress ( $\sigma^*$ ) decreases until a flat region with a decline of the reciprocal of the extension ratio ( $\lambda^{-1}$ ), and then rises again. The  $\lambda^{-1}$  value at the upturn point implies finite extensibility of the polymer chains while stretching.<sup>27</sup> With a better reinforcement (i.e. higher degree of filler-polymer coupling), the length of bridging polymer chains between adjacent filler particles becomes short and restricted, thus contributes to the modulus. Therefore, the  $\lambda^{-1}$  value at the upturn point can be used as an indicator for the intensity of filler-polymer interaction as well as the crosslink network. By using mathematical software, the  $\lambda^{-1}$  value where the slope of the tangential line of the Mooney-Rivlin plot becomes zero was selected as the  $\lambda^{-1}$  value at the upturn point.

## RESULTS AND DISCUSSION

### FILLER-FILLER INTERACTION (PAYNE EFFECT) AS A FUNCTION OF SBR CONTENT

The Payne effect values of the uncured compounds of the pre-blend and masterbatch in Series 1 are plotted as a function of SBR content in Figure 2.

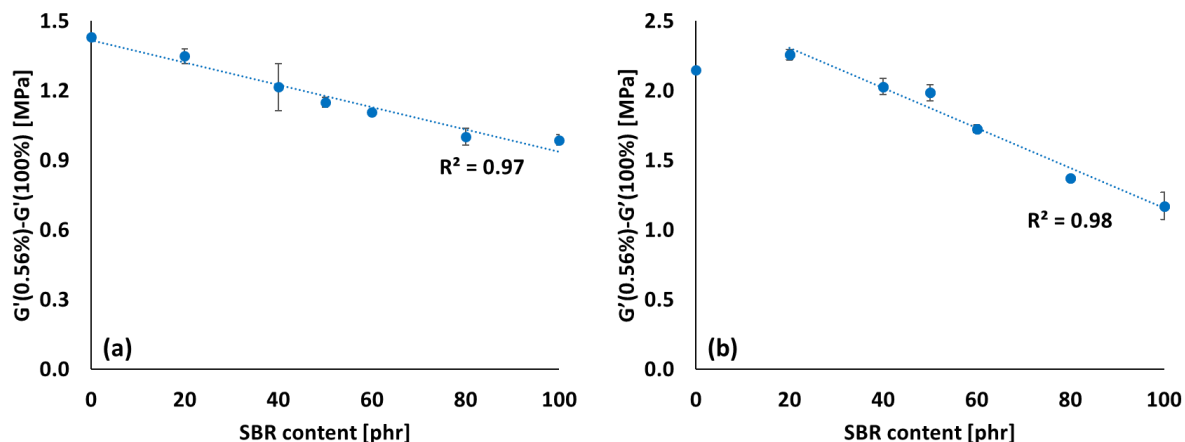


Figure 2 Payne effect as a function of SBR content; (a): pre-blending; (b): masterbatch.

Pre-blended compounds – containing 50 phr of silica – show a decreasing Payne effect value with increasing SBR content, even though there was no silane present at all: Figure 2(a). This trend indicates that the affinity or surface wetting behavior of SBR towards silica is better than BR, as also reported by Le et al. and Wang and Wolff.<sup>5-8</sup> Masterbatch compounds – containing 100 phr of silica and 8.4 phr of silane – also show a lower Payne effect value with increasing SBR content except for SBR00, which contains only BR. This trend can be explained with the affinity or surface wetting behavior of SBR; however, it is better interpreted with bound rubber content which will be discussed next.

### THE EFFECT OF SILICA DISPERSIBILITY ON MACRO- AND MICRO-DISPERSION

In Series 2, the compounds without silane (COM1 and 2), the dispersibilities of the silicas are compared in terms of macro- and micro-dispersion after mixing, and the results are depicted in Figure 3. Surprisingly, the

Payne effect levels were almost the same for both silicas: Figure 3(b). However, a significant difference was observed in the macro-dispersion. As can be seen in Figure 5.3(a), HD silica shows a much better dispersibility in terms of macro-dispersion.

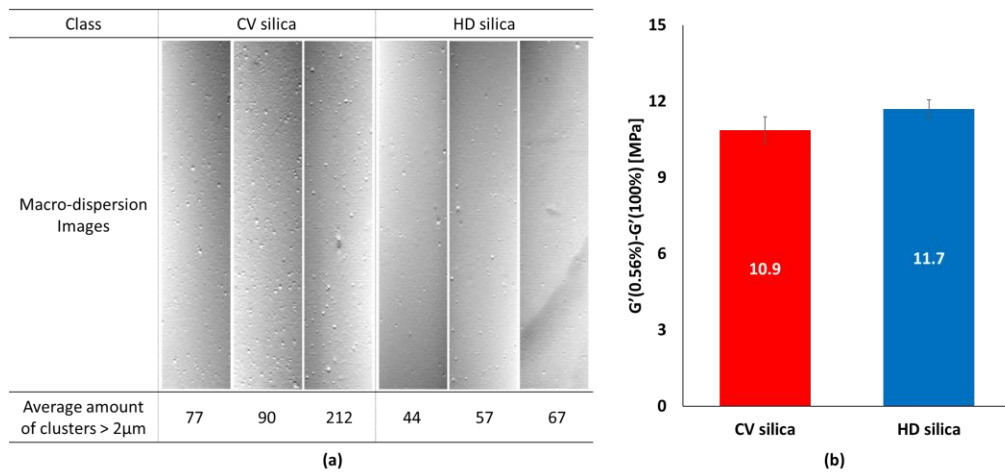


Figure 3 Dispersibility comparison of the silicas of COM1 and COM2; (a): macro-dispersion; (b): Micro-dispersion represented by the Payne effect; (■): CV silica; (■): HD silica.

For the compounds containing silane (COM3 and 4), similar micro-dispersion results are obtained. As shown in Figure 4(b), the levels of the Payne effect – representing the degree of micro-dispersion – is plotted as a function of silanization time. However, the type of silica does not affect the micro-dispersion.

Concerning the macro-dispersion level, a significant difference between the silicas is obtained (Figure 4(a)), similar to the case when no silane is used as illustrated in Figure 3(a): A better macro-dispersion quality is obtained for HD silica. However, the presence of silane as well as a longer silanization time does not affect the degree of macro-dispersion. These results indicate the mutual independence of macro- and micro-dispersion of the respective silicas in the rubber matrix.<sup>32</sup>

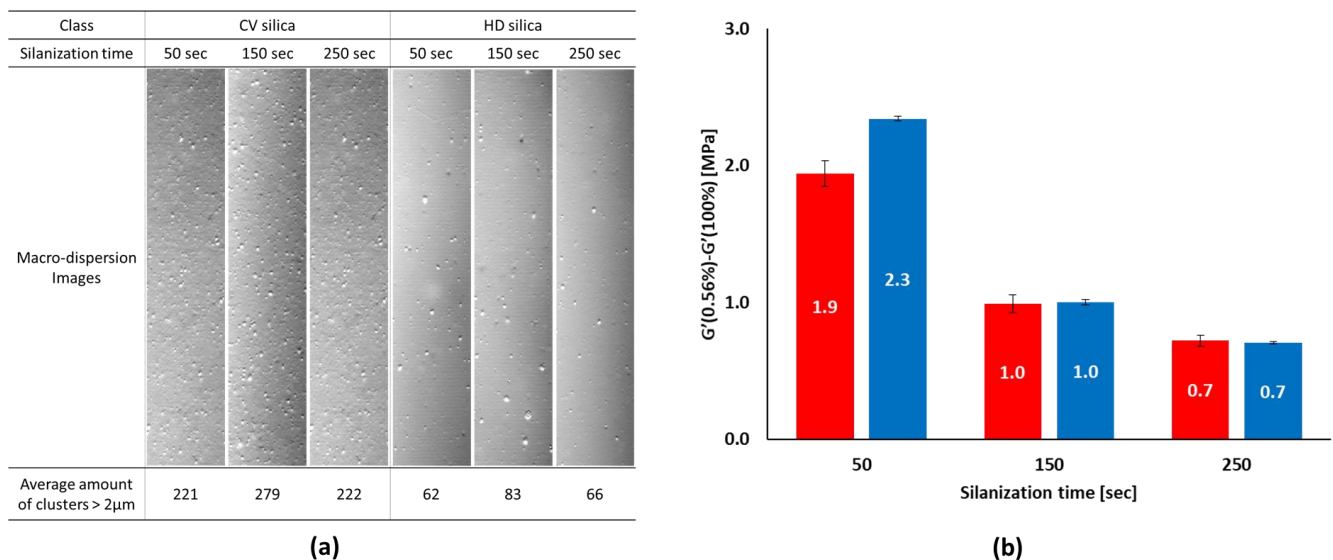


Figure 4 Dispersibility comparison of the silicas of COM3 and COM4; (a): macro-dispersion;

(b): micro-dispersion represented by the Payne effect; (■): CV silica; (■): HD silica.

#### BOUND RUBBER CONTENT AS A FUNCTION OF SBR CONTENT

Figure 5 shows the amount of bound rubber of masterbatch compounds as a function of SBR content. Except for SBR00 (0 phr of SBR, full BR), an increasing amount of total and chemically bound rubber is observed when the SBR content increases.

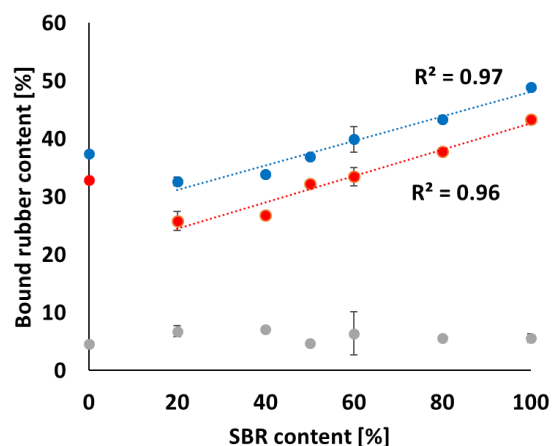


Figure 5 Bound rubber content as a function of SBR content; (●): total bound rubber; (●): chemically bound rubber; (●): physically bound rubber.

This result can be explained with the high reactivity of vinyl groups in S-SBR and thiol radicals generated from the silane (TESPT). Sato compared the reactivity between sulfidic silane and model olefins – representing the vinyl group in SBR and cis as well as trans double bonds in SBR and BR – and found that the vinyl group is the most reactive moiety.<sup>33</sup> The reaction between a double bond (ene) and a thiol radical – thiol-ene click reaction – is well known for its rapid rate and high efficiency of the reaction.<sup>34-37</sup>

#### BOUND RUBBER CONTENT AS A FUNCTION OF SILANIZATION TIME

The amount of bound rubber of COM3 and 3 in Series 2 is shown in Figure 6. In this figure, the amounts of bound rubber are plotted as a function of silanization time: a slightly higher amount of total and chemically bound rubber are obtained for the compounds with CV silica due to the slightly higher amount of silane according to the surface area: 0.7 phr of silane was additionally added to the CV silica compound compared to the HD silica containing one. Figures 5 and 6 again give indication that the dispersibility of the silicas shows almost no effect on the amount of bound rubber. Jin et al. reported that the amount of bound rubber is mainly affected by the degree of silanization, and the silanization time turned out to be one of the key factors for the efficiency of the silanization reaction. Therefore, equal silanization temperatures and times lead to similar kinetics of silanization for both compounds, independent of the type of silica.

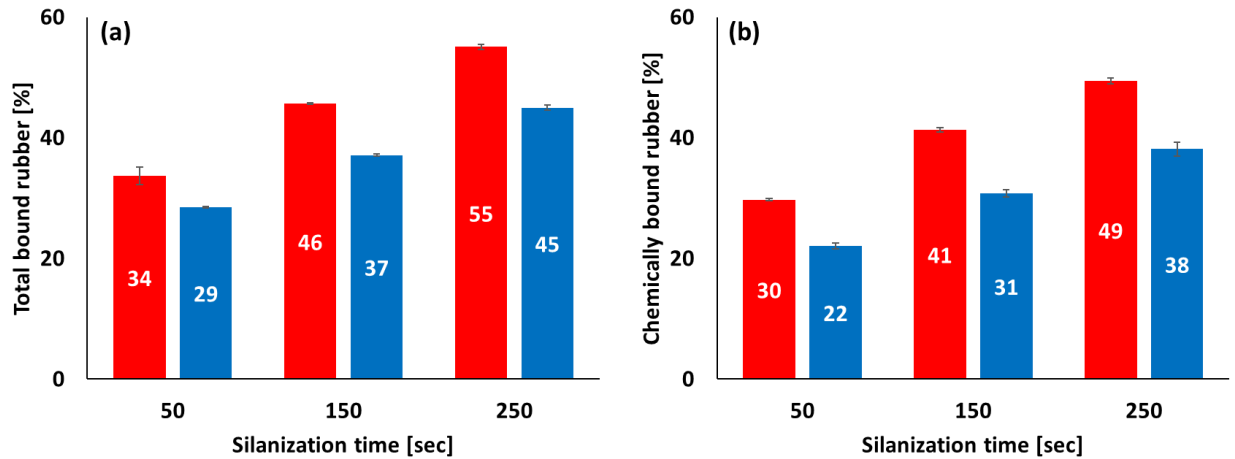


Figure 6 Amounts of bound rubber; (a): total bound rubber; (b): chemically bound rubber; (■): CV silica; (■): HD silica.

#### SILICA FILLER FLOCCULATION RATE AND FILLER-POLYMER COUPLING RATE AS A FUNCTION OF POLYMER BLEND RATIO

The silica Filler Flocculation Rates (FFR) and the filler-polymer Coupling Rates (CR) of Series 1 are shown in Figure 7(a) and 7(b) respectively. The FFR values increase until the SBR/NR blend ratio reaches 50/50. Different from FFR result, CR plotted as a function of SBR content show an increasing trend with SBR content.

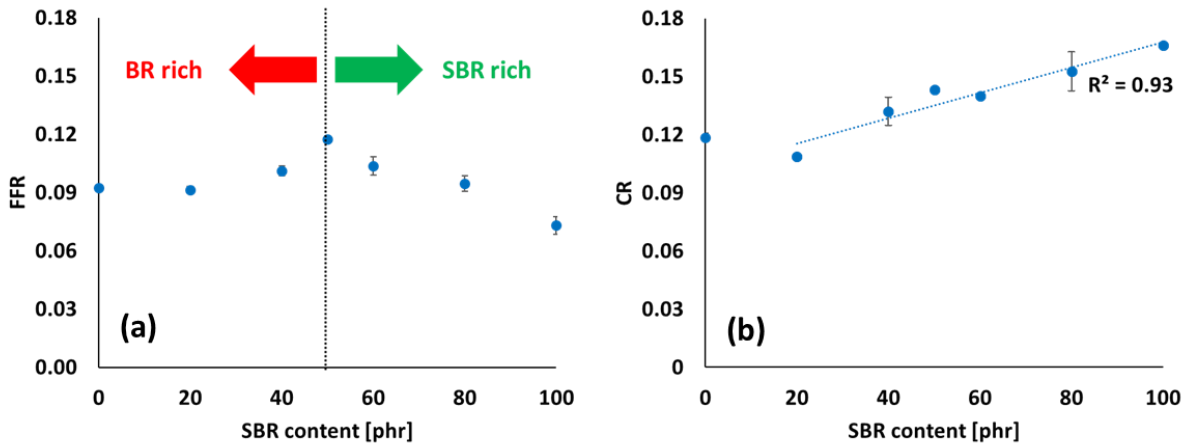


Figure 7 FFR vs. SBR content.

*Silica filler flocculation rate of Series 1.*— These results can be explained by a filler re-localization process.<sup>5,38-41</sup> Reinforcing fillers such as silica can be localized in one blend phase or at the interphase between the two components.<sup>38,39</sup> Le et al. reported that filler transfer occurs from a less preferred blend phase into which silica was introduced by the mixing process to the more favorable one.<sup>5</sup> A model of filler localization for silica filled compounds with 100% SBR, SBR rich, BR rich and 100% BR based on the results of this work is suggested in Figure 8.

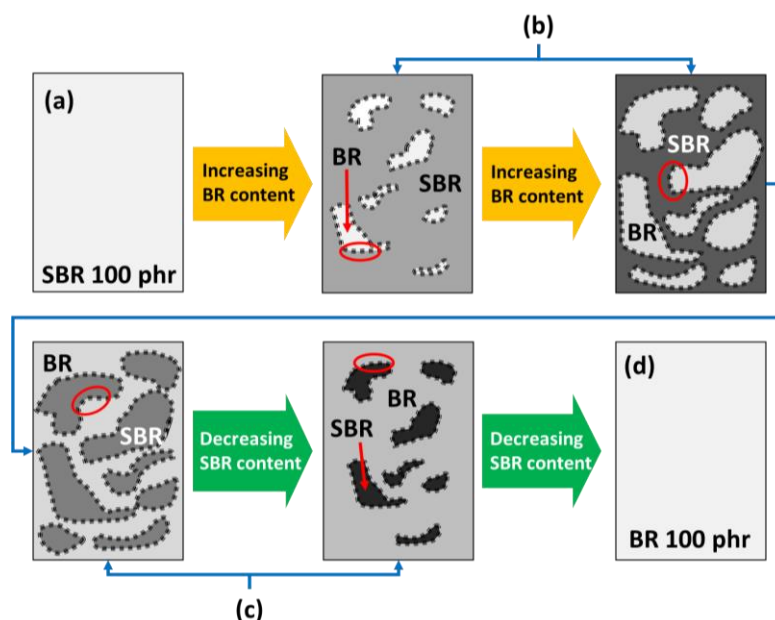


Figure 8 Filler localization model; (a): SBR 100%; (b): SBR rich; (c): BR rich; (d): BR 100%; (○): filler localized at the interphase of SBR and BR; the population of silica is expressed by the color; darker color represents higher population of silica.

In the extreme cases (with 100 phr SBR or BR, Figure 8(a) and Figure 8(d)), silica has no alternative than the matrix of the respective polymer, therefore the silica clusters will be first distributed more homogeneously during mixing compared to a matrix with SBR or BR rich regions. When these compounds undergo the FFR measurements, the clusters will start to flocculate without any other effects induced by the immiscibility of SBR and BR. Due to the fact that the physical affinity of silica towards BR is lower compared to SBR, silica would flocculate slightly faster for the compound with 100% of BR.<sup>6</sup> Figure 7(a).

In the case of the SBR rich region (Figure 8(b)), the silica localized in the BR phase or at the interphase of BR and SBR tends to migrate to the SBR phase, the preferred one for silica in this system. Increasing the BR content enhances the migration of silica to SBR, as a higher percentage of the total amount of silica is present in the BR phase or at the interphase of BR and SBR due to the higher amount of BR compared to SBR. Additionally, a smaller SBR volume (dark area in Figure 8(b)) induced by increasing BR content would result in a shorter distance between silica clusters in this phase. As a consequence, silica flocculation will be enhanced.

The same phenomenon will take place for the BR rich region as well (Figure 8(c)). In the BR rich region, the migration of the silica from the BR phase or the BR/SBR interphase into the SBR phase is blocked, when the silica incorporation capacity of the SBR phase reaches its limit. The absolute maximum silica incorporation capacity of the SBR phase decreases as the SBR content in the BR rich region becomes lower. As a consequence, the flocculation of silica mainly occurs in the BR phase or at the SBR/BR interphase.

*Filler-polymer coupling rate of Series 1.* – Increasing the amount of SBR in the compound formulation leads to a higher concentration of vinyl groups and thus to an enhancement of the thiol-ene click reaction. This result is another indication for the thiol-ene click reaction between the vinyl groups of SBR and the sulfur radicals generated from TESPT: when more vinyl groups are present, enhanced filler-polymer coupling via the sulfidic silane is occurring. Therefore, a higher amount of chemically bound rubber is obtained when the content of SBR increases as was seen in Figure 5.

### SILICA FILLER FLOCCULATION RATE AND FILLER-POLYMER COUPLING RATE AS A FUNCTION OF SILANIZATION TIME

In Series 2, the FFR and CR decrease when a longer silanization time is applied for the compounds: Figure 9. When the macro-dispersion results (Figure 4(a)) are also taken into account, it can be concluded that the FFR and CR are mainly influenced by the degree of silanization, regardless of the dispersibility of the silicas or the degree of macro-dispersion of the compounds: these rates decrease with increasing silanization time, whereas the macro-dispersion (Figure 4(a)) is not influenced.

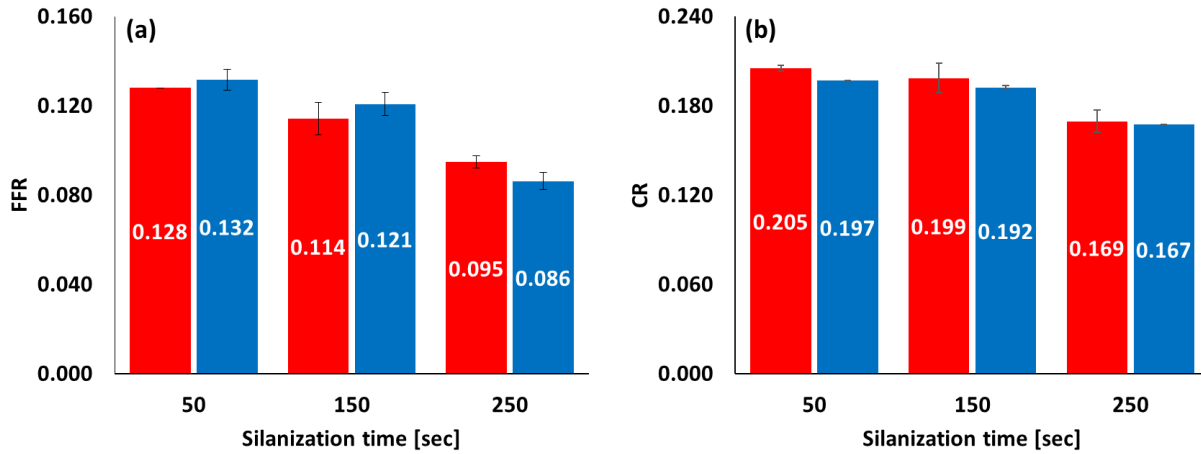


Figure 9 FFR and CR as a function of silanization time; (a): FFR; (b): CR; (■): CV silica; (■): HD silica.

### MARCHING MODULUS INTENSITY

The Marching Modulus Intensity (MMI) measured at small (ASTM Conditions, MMI 0.5) strains of all mixing series are plotted in Figure 10.

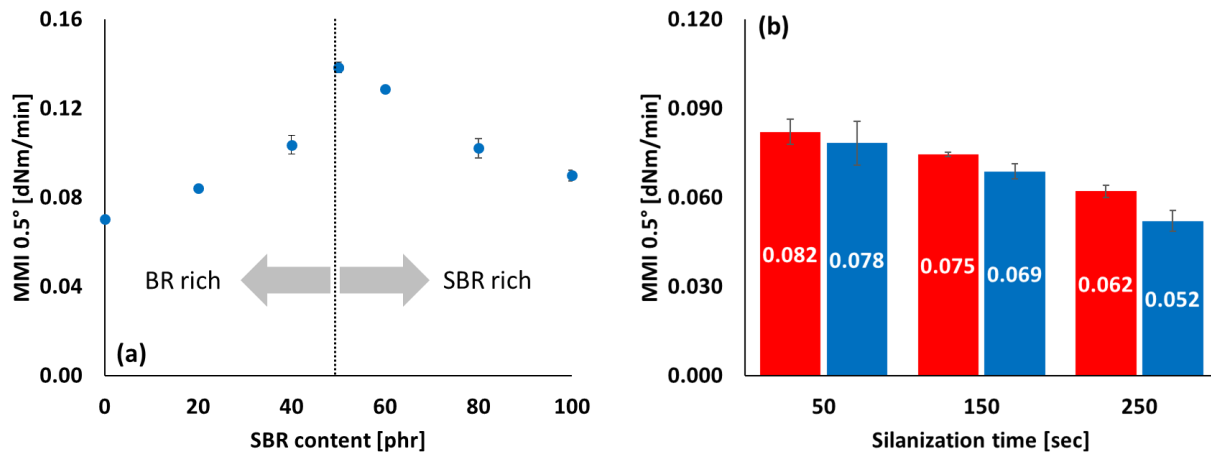


Figure 10 MMI of samples in all series; (a): MMI vs. SBR content (Series 1); (b): MMI vs. silanization time (Series 2); (■): CV silica; (■): HD silica.

*MMI 0.5° of Series 1.*— As can be seen in Figure 10(a), the MMI 0.5° values corresponding to the SBR contents show a similar trend as the FFR trend. Taken from Figure 7(a) and Figure 10(a), the MMI 0.5° values of the BR rich and SBR rich regions are plotted as functions of FFR and depicted in Figure 11. Both polymer regions show positive correlations. These results indicate that the silica filler flocculation behavior in the rubber

matrix is still the strongly influencing factor for MMI 0.5°. However, the driving force of silica flocculation in this case should be distinguished from that of the compounds reported by Jin et al.:<sup>22</sup> the amount of chemically bound rubber. The reason is that in the results of Jin et al., the compound formulation was fixed and the only variable was the mixing temperature. In the present case, FFR is affected not only by the amount of chemically bound rubber but also by the re-localization or migration of silica between the rubber phases induced by the different polymer blending ratios.

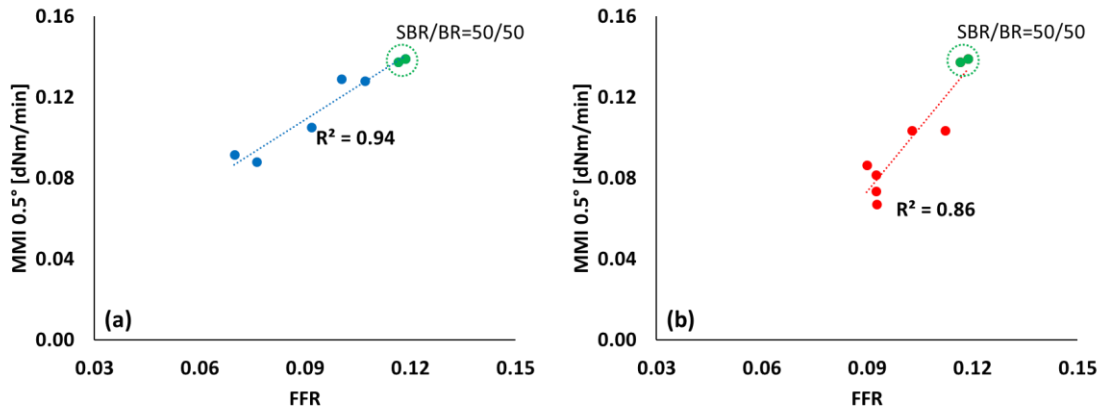


Figure 11 MMI 0.5° as a function of FFR; (a): SBR rich; (b): BR rich; (●): SBR/BR=50/50.

Compared to the results of Jin et al., another difference can be found in the present study: the CR does not affect the MMI 0.5°, Figure 12. In order to explain this phenomenon, the mechanism of the reaction of filler-polymer coupling via the silane coupling agent and sulfur curing as well as the formulations of the masterbatch and final compounds need to be taken into account.

CR was measured on the masterbatch, which means that there were no accelerators present such as such CBS and ZBEC. In the case of the masterbatch compound, therefore, higher values of CR were obtained with increasing the SBR content due to the increasing vinyl groups concentration: Figure 7(b).

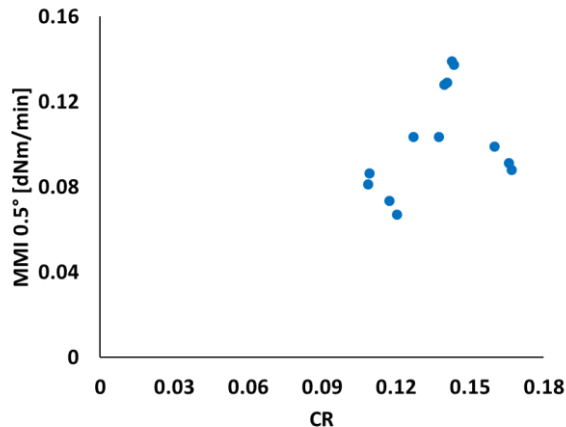


Figure 12 MMI 0.5° vs. CR.

However, the final compounds do contain accelerators (CBS and ZBEC). Sato compared the reaction between a model olefin – representing the vinyl groups of SBR – and a sulfidic silane with and without CBS.<sup>33</sup>



He found that the model olefin and the sulfidic silane do not react in the presence of CBS: the silane tends to incorporate more sulfur into its structure rather than reacting with the model olefin. Sato's results indicate that filler-polymer coupling by vinyl groups of the SBR will not occur to a large extent during curing of the final compound containing CBS.

Klockmann et al. stated that, once the silane is coupled to the silica, the silane can be stabilized and react further with the polymer after forming a silica-silane-CBS intermediate:<sup>43</sup> Figure 13.

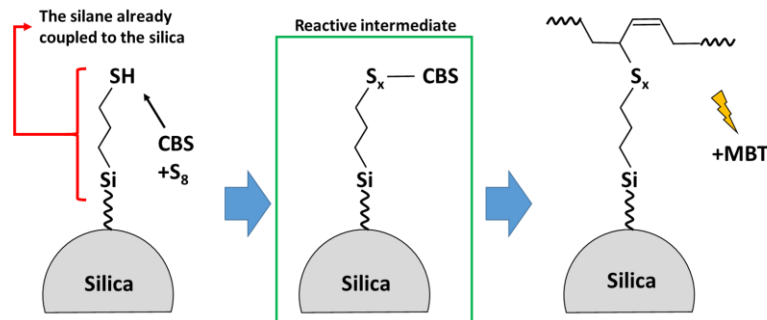


Figure 13 Immobilization mechanism of a mercapto-silane reacting with CBS: preventing dimerization of the silane.<sup>42,43</sup>

Overall, these results indicate that the filler-polymer coupling via a silane during vulcanization of the final compound can differ from the reaction taking place during masterbatch mixing, as the latter contains the accelerators, which can interfere with the silane-polymer reaction. The vinyl group can react with the silane via an intermediate reaction with CBS; however, the reaction rate would be slower than the rate of the thiol-ene click reaction without CBS. Therefore the CR obtained from the masterbatch compound hardly affects the MMI in the latter case: Figure 12.

*MMI 0.5° of Series 2.*— Compared to CV silica, HD silica shows slightly lower MMI 0.5° values due to a smaller specific surface area and thus a lower amount of silanol groups in this case. A similar tendency depending on the specific surface area of silica can be found in Mihara's work.<sup>28</sup> A longer silanization time leads to a lower MMI 0.5° due to a reduced FFR and CR. The dispersibility of the silicas as well as the degree of macro-dispersion of the compounds show no effect on MMI 0.5°.

### SBR/BR BLEND RATIO VS. CURING BEHAVIOR

In the rheograms of the compounds in Series 1 measured at large strain (Figure 14), an interesting point can be seen in the beginning of the vulcametry: a steeper slope at the initial part of the rheogram (maximum cure rate) is found when the SBR content decreases or the BR content increases.

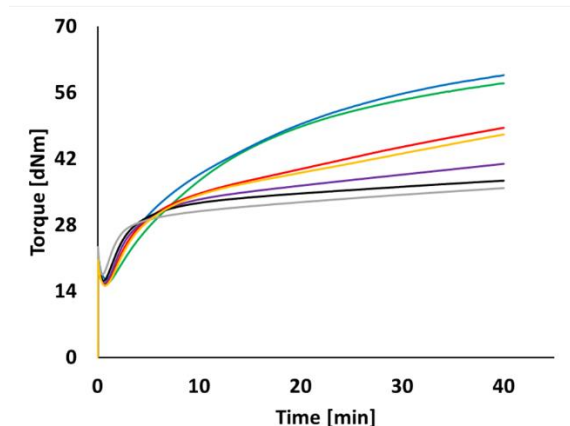


Figure 14 Rheograms of the compounds in Series 1 at large (~42%) strain; ( — ): SBR100; ( — ): SBR80; ( — ): SBR60; ( — ): SBR50; ( — ): SBR40; ( — ): SBR20; ( — ): SBR00.

The maximum cure rate for the compounds and the time when the compounds show the maximum cure rate were calculated by differentiating the rheograms (Figure 14) and are shown in Figure 15(a). A higher maximum cure rate is observed when the amount of BR increases: Figure 15(b). Additionally, the times at which the maximum cure rate is reached are longer when the amount of SBR increases: Figure 15(c). Dogadkin et al. compared the reactivity between sulfur and double bonds of the 1,4- and 1,2-configurations (vinyl) of BR and found that the reactivity of the 1,4-carbon-carbon double bond is higher than the reactivity of the 1,2-double bond.<sup>44</sup> Figure 16. Similarly, Marzocca et al. obtained a higher crosslink density when the amount of cis BR increases in the blend.<sup>1</sup>

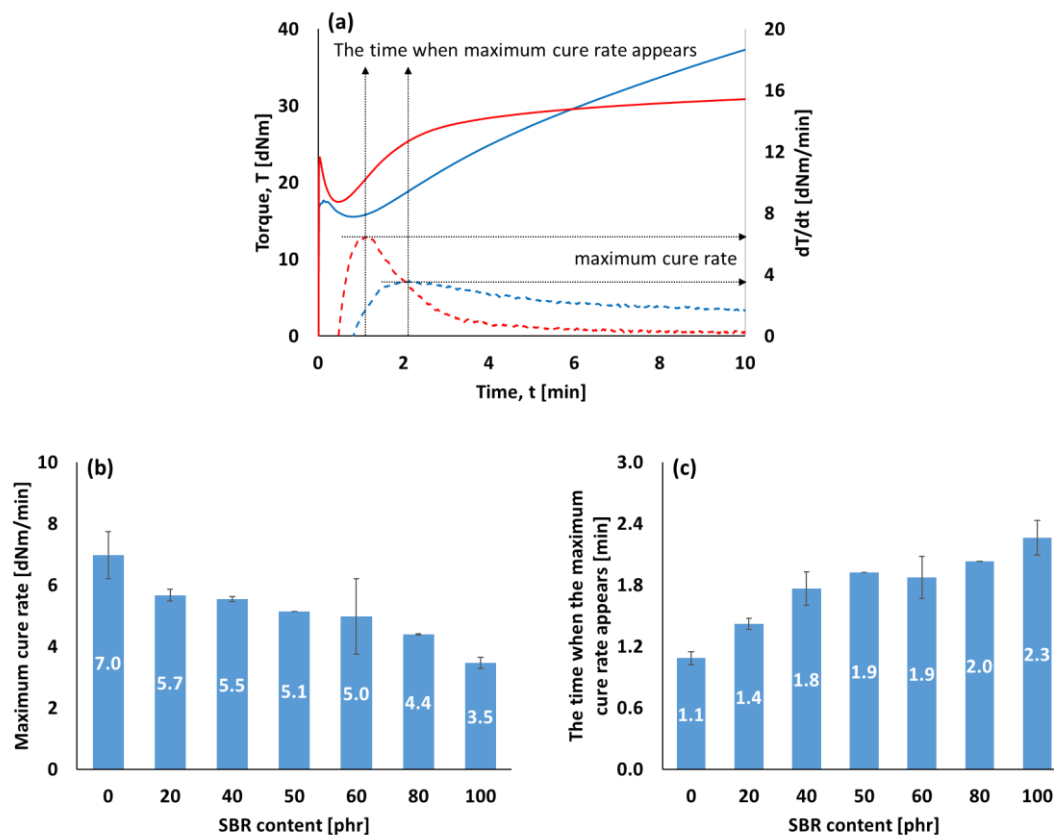


Figure 15 Calculated maximum cure rate and time to reach the maximum cure rate based on Figure 13(b); (a): example rheograms for SBR100 and SBR00 at large strain and their differential curves; (solid lines): Torque; (dotted lines):  $dT/dt$ ; ( — ): SBR100; ( — ): SBR00; (b): maximum cure rate; (c): time to reach the maximum cure rate.

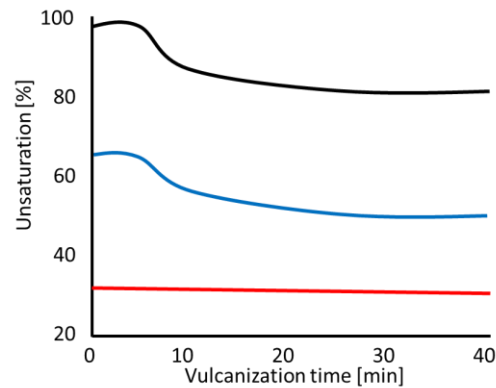


Figure 16 Variation of the unsaturation of rubber with 65% of 1,4 structural units during vulcanization in film form in a nitrogen atmosphere at 142°C; ( — ): total unsaturation; ( — ): unsaturation of 1,4-structure; ( — ): unsaturation of 1,2-structure.<sup>44</sup>

In order to confirm this interpretation, the crosslink density of the vulcanizates with two different curing times – Calculated Curing Time (CCT, listed in Table VII) and 30 minutes – were compared by measuring swelling ratios: Figure 17. As can be seen in this figure, the swelling ratios of the vulcanizates cured for the calculated time increase along with SBR content. As higher swelling ratio values correspond to lower crosslink densities, the SBR rich compounds have a lower crosslink density than the BR rich ones. Even though the SBR00 compound (100 phr of BR) was cured for the shortest curing time (about half the time of the SBR100 compound), it shows the highest crosslink density.

Table VII Calculated curing times.

SBR content [phr]	Calculated curing time [min]
100	11.7
80	11.6
60	9.8
50	9.2
40	8.2
20	6.5
00	6.2

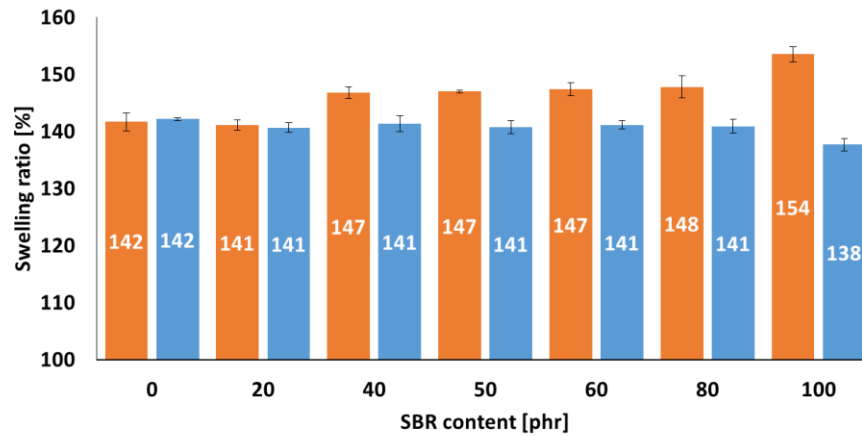


Figure 17 Swelling ratios of the vulcanizates with; (■): calculated curing time; (■): 30 minutes.

Finally the crosslink densities of all compounds become similar after 30 minutes of curing. Additionally, another interesting point can be seen in Figure 14: the maximum torque – taken as the torque at 40 minutes ( $T_{40}$ ) – becomes higher when the SBR content increases. This result indicates that more filler-polymer coupling takes place in the SBR rich compounds on a longer time range. Limited polymer chain extensibility as evaluated by the Mooney-Rivlin equation, gives another evidence for more filler-polymer coupling of the compounds containing large amount of SBR. As can be seen in Figure 18,  $\lambda^{-1}$  at the upturn point increases along with the SBR content. In particular SBR100 shows a large difference in  $\lambda^{-1}$  at the upturn point between the two curing times, which means that more filler-polymer coupling occurred during vulcanization.

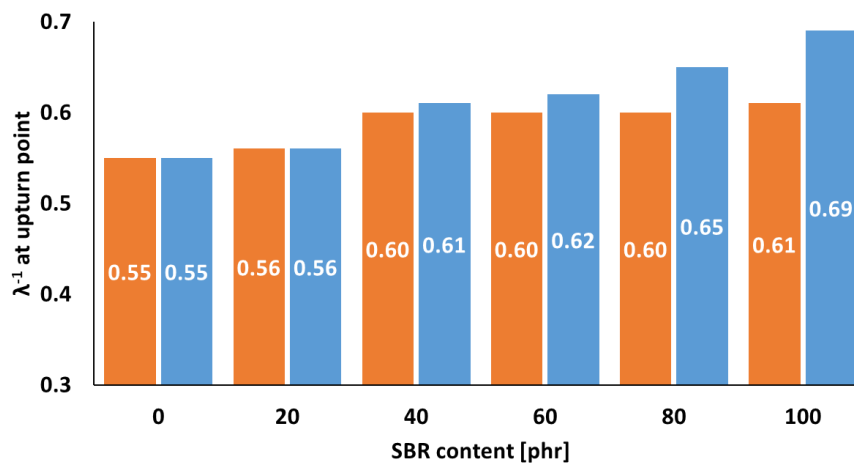


Figure 18  $\lambda^{-1}$  at the upturn point of the vulcanizates with; (■): calculated curing time; (■): 30 minutes.

Taking into account Figures 7(b), 14, 15, 17 and 18, the following can be deduced:

- The 1,4-structure double bond in SBR and BR is more reactive for sulfur curing than the 1,2-vinyl configuration. As a consequence, the compounds with a large amount of BR (having 96% of 1,4-cis content) show a higher increment of torque in the beginning of the rheogram than SBR rich compounds;

- The presence of a curing accelerator such as CBS, suppresses the reaction between the sulfidic silane and the 1,2-structure double bond of SBR. However, the reaction still can happen on a long time range as indicated by a higher MMI 3°;
- The slow filler-polymer coupling reaction during the vulcanization process of SBR rich compounds results, however, in more crosslinks between filler and polymer: a higher torque level at 40 minutes of the rheogram measurement.

## CONCLUSIONS

In Series 1, the effect of the polymer (SBR/BR) blend ratio on the marching modulus intensity of a silica filled compound was investigated. The polymer blend ratio turned out to be a strong influencing factor for the marching modulus as well as for the other curing characteristics.

The MMI 0.5° of the compounds having different SBR/BR blend ratios is mainly affected by the silica flocculation rate. The FFR in the BR rich region is not affected by the amount of bound rubber, but influenced by the chemical characteristics of the rubber and silica. The silica tends to migrate to and be localized in the more preferred rubber phase (SBR). However, when the incorporation capacity of the favorable elastomer phase reaches its maximum, silica migration and, as a consequence, flocculation slows down.

The filler-polymer coupling reaction is strongly affected by the SBR content and the presence of an accelerator such as CBS. For the masterbatch compounds, increasing percentages of SBR lead to higher CR values due to a thiol-ene click reaction. But as soon as CBS is added to the compound in the final mixing step, the reaction rate slows down. Therefore, MMI 0.5° of the compounds were not affected by the CR.

The reactivity of the 1,4- and the 1,2-structure double bonds towards formation of sulfur bonds between the filler and polymer influences the rheogram and MMI at large strain. The 1,4-double bonds in SBR and BR are more reactive than 1,2-double bonds in sulfur curing. Due to the reactivity of these types of double bonds, faster vulcanization is observed for BR rich compounds. However, the slow filler-polymer coupling reaction during the vulcanization process for the SBR rich compounds results in more crosslinks as the cure time increases: decrease in the swelling ratio and increase in  $\lambda^{-1}$  at the Mooney-Rivlin upturn point of the vulcanizates along with cure time. As a consequence, a higher torque level after 40 minutes curing as well as MMI 3° were obtained.

In Series 2, the effect of dispersibility of two different silicas on the marching modulus phenomenon was investigated. The results indicate, that the dispersibility of silica has no effect on the curing behavior of silica filled rubber.

None of the factors related to the MMI 0.5° – filler-filler interaction, the amount of bound rubber, FFR and CR – was influenced by the dispersibility of the silicas or by the degree of macro-dispersion of the compounds. The specific surface area can affect the MMI 0.5°, however this effect was found to be small.

The dispersibility of silica is strongly related to the degree of macro-dispersion of the compounds, but not to the degree of micro-dispersion nor to the efficiency of the silanization reaction.

## ACKNOWLEDGEMENT

The authors gratefully acknowledge financial and in-kind support from HANKOOKTIRE CO., LTD. Main R&D Center (Daejeon, Korea), Evonik Resource Efficiency GmbH (Wesseling, Germany) and Solvay (Lyon, France).

## REFERENCES

- [1] A. J. Marzocca, S. Cervený, J. M. Méndez, *Polym. Int.* **49**, **2000**, 216.
- [2] J. M. Massie, R. C. Hirst, A. F. Halasa, *RUBBER CHEM. TECHNOL.* **66**, **1993**, 276.
- [3] J. E. Callan, W. M. Hess, C. E. Scott, *RUBBER CHEM. TECHNOL.* **44**, **1971**, 814.
- [4] T. Inoue, F. Shomura, T. Ougizawa, K. Miyasaka, *RUBBER CHEM. TECHNOL.* **58**, **1985**, 873.
- [5] H. H. Le, M. Keller, M. Hristov, S. Ilisch, T. H. Xuan, Q. K. Do, T. Pham, K-W. Stöckelhuber, G. Heinrich, H-J. Radusch, *Macromol. Mater. Eng.* **298**, **2013**, 1085.
- [6] M. J. Wang, S. Wolff, J. B. Donnet, *RUBBER CHEM. TECHNOL.* **64**, **1991**, 714.
- [7] H. H. Le, S. Ilisch, D. Heidenreich, K. Osswald, H-J. Radusch, *RUBBER CHEM. TECHNOL.* **84**, **2011**, 41.
- [8] H. H. Le, S. Ilisch, D. Heidenreich, A. Wutzler, H-J. Radusch, *Polym. Compos.* **31**, **2010**, 1701.
- [9] K. W. Stöckelhuber, A. S. Svistkov, A. G. Pelevin, G. Heinrich, *Macromolecules* **44**, **2011**, 4366.
- [10] L. Tadiello, M. D'Arienzo, B. Di Credico, T. Hanel, L. Matejka, M. Mauri, F. Morazzoni, R. Simonutti, M. Spirkovac, R. Scotti, *Soft Matter* **11**, **2015**, 4022.
- [11] J. Fröhlich, W. Niedermeier, H. D. Luginsland, *Composites Part A* **36**, **2005**, 449.
- [12] J. L. Leblanc, *Prog. Polym. Sci.* **27**, **2002**, 627.
- [13] R. Scotti, L. Wahba, M. Crippa, M. D'Arienzo, R. Donetti, N. Santo, F. Morazzoni, *Soft Matter* **8**, **2012**, 2131.
- [14] L. Wahba, M. D'Arienzo, R. Donetti, T. Hanel, R. Scotti, L. Tadiello, F. Morazzoni, *RSC Adv.* **3**, **2013**, 5832.
- [15] F. Grunert, A. Wehmeier, A. Blume, 12th Fall DIK Rubber Colloquium, Hannover, Germany, 22-24 November, Paper No. 21 (2016).
- [16] A. Blume, S. Uhrlandt, 157th meeting ACS Rub. Div., Dallas, Texas, Paper No. 32 (2000).
- [17] F. Grunert, PhD thesis: Analytical Method Development to Predict the In-Rubber Dispersibility of Silica, Univ. Twente: Enschede, the Netherlands (2018).
- [18] L. Guy, S. Daudey, P. Cochet, Y. Bomal, *Kautsch. Gummi Kunstst.* **63**, 383 (2009).
- [19] ASTM D2663-14, "Standard Test Method for Carbon Black – Dispersion in Rubber, Test Method C – Microroughness Measurement with Profilometer", ASTM International (2015).
- [20] S. Mihara, R. N. Datta, J. W. M. Noordermeer, *RUBBER CHEM. TECHNOL.* **82**, **2009**, 524.
- [21] Factors reducing the marching modulus of silica filled tire tread compounds; J. Jin, J. W. M. Noordermeer, W. K. Dierkes, A. Blume, poster 28 at the Deutsche Kautschuk-Tagung, Nuremberg, Germany, 2-5 (July, **2018**).
- [22] The origin of marching modulus of silica-filled tire tread compounds; J. Jin, J. W. M. Noordermeer, W. K. Dierkes, A. Blume, *RUBBER CHEM. TECHNOL.* DOI:10.5254/rct.19.80453
- [23] Standard Test Method for Rubber Property—Vulcanization Using Rotorless Cure Meters; *ASTM Standard D5289-95*, ASTM International, **2001**.
- [24] S. Wolff, M. J. Wang, E-H. Tan, *RUBBER CHEM. TECHNOL.* **66**, **1993**, 163.
- [25] Reactive processing of silica-reinforced tire rubber: new insight into the time- and temperature-dependence of silica rubber interaction; S. Mihara, *PhD Thesis*, University of Twente, May, **2009**.
- [26] C. Hayichelaeh, L. A. E. M. Reuvekamp, W. K. Dierkes, A. Blume, J. W. M. Noordermeer, K. Sahakaro, *RUBBER CHEM. TECHNOL.* **91**, **2018**, 433.
- [27] L. Bokobza, *Macromol. Mater. Eng.* **289**, **2004**, 607.
- [28] The Physics of Rubber Elasticity, 3rd Edition; L. R. G. Treloar, *Oxford University Press*, NY, USA **1975**.
- [29] Y. Zhan, J. Wu, H. Xia, N. Yan, G. Fei, and G. Yuan, *Macromol. Mater. Eng.* **296**, **2011**, 590.
- [30] B. Zhong, Z. Jia, D. Hu, Y. Luo, and D. Jia, *Composites Part A* **78**, **2015**, 303.
- [31] Z. Tang, J. Huang, X. Wu, B. Guo, L. Zhang, and F. Liu, *Ind. Eng. Chem. Res.* **54**, **2015**, 10747.
- [32] J. Jin, W. Kaewsakul, J.W.M. Noordermeer, W.K. Dierkes, A. Blume, International Rubber Conference, London, United Kingdom, 3-5 September (2019).
- [33] Reinforcing mechanisms of silica / sulfide-silane vs. mercapto-silane filled tire tread compounds; M. Sato, *PhD thesis*, University of Twente, July, **2018**.
- [34] T. Posner, *Ber. Dtsch. Chem. Ges.* **38**, **1905**, 646.
- [35] M. S. Kharasch, A. T. Read, F. R. Mayo, *Chem. Ind.* **57**, **1938**, 752.

- [36] C. R. Morgan, F. Magnotta, A. D. Ketley, *J. Polym. Sci. Polym. Chem. Ed.* **15**, **1977**, 36 627.
- [37] C. E. Hoyle, T. Y. Lee, T. Roper, *J. Polym. Sci. Part A* **42**, **2004**, 5301.
- [38] M. Sumita, K. Sakata, S. Asai, K. Miyasaka, H. Nakagawa, *Polym. Bull.* **25**, **1991**, 265.
- [39] M. Sumita, K. Sakata, Y. Hayakawa, S. Asai, K. Miyasaka, M. Tanemura, *Colloid Polym. Sci.* **270**, **1992**, 134.
- [40] A. E. Zaikin, R. R. Karimov, V. P. Arkhireev, *Colloid J.* **63**, **2011**, 53.
- [41] A. E. Zaikin, E. A. Zharinova, R. S. Bikmullin, *Polym. Sci. Ser. A* **49**, **2007**, 328.
- [42] O. Klockmann, J. Hahn, H. Scherer, International Rubber Conference 2009, Nuremberg, Germany, June 29-July 2, **2009**.
- [43] B. A. Dogadkin, D. L. Fedyukin, V. E. Gul, *RUBBER CHEM. TECHNOL.* **31**, **1958**, 756.